The impact of convective cold pool outflows on model biases in the Sahara

L. Garcia-Carreras,[1] J. H. Marsham,[1,2] D. J. Parker,[1] C. L. Bain,[3] S. Milton,[3] A. Saci,[4] M. Salah-Ferroudj,[4] B. Ouchene,[4] and R. Washington[5]

Received 15 November 2012; revised 6 February 2013; accepted 2 June 2013; published 26 April 2013.

[1] Radiosonde data from Fennec supersite-1 in the remote central Sahara have been used to evaluate the impact of convectively generated cold pool outflows on model errors. Model predictions are too warm and dry, with cold pools contributing significantly to the mean bias. Although dust concentrations are high within cold pools, the sign of the errors is inconsistent with radiative impacts of dust. Cold pools cause 29% of the meridional humidity flux, but this contribution is absent in the forecast and analysis. Assimilating radiosondes reduces the errors, but significant temperature and meridional humidity flux biases remain at night. The model biases are consistent with the larger-scale heat low biases in the operational Met Office Unified Model and can be linked to known issues with convective parameterizations used in all global weather and climate models. This study suggests that the misrepresentation of moist convective processes can affect continental-scale biases, altering the West African monsoon circulation.
Citation: Garcia-Carreras, L., J. H. Marsham, D. J. Parker, C. L. Bain, S. Milton, A. Saci, M. Salah-Ferroudj, B. Ouchene, and R. Washington (2013), The impact of convective cold pool outflows on model biases in the Sahara, *Geophys. Res. Lett.*, *40*, 1647–1652, doi:10.1002/grl.50239.

1. Introduction

[2] The Saharan heat low (SHL) is formed in the summer as a result of high insolation, low surface evaporation, and large-scale subsidence in the descending part of the Hadley circulation. The SHL is a major element of the West African monsoon (WAM), strengthening the moist monsoon flow on its western and southern flanks, and the dry Harmattan flow in the north and east [*Parker et al.*, 2005]. The development of the SHL is also linked to the monsoon onset [*Ramel et al.*, 2006], the timing of which is critical for a large proportion of the Sahelian population that depends on rain-fed agriculture.

All supporting information may be found in the online version of this article.

[1]School of Earth and Environment, University of Leeds, Leeds, UK.
[2]National Centre for Atmospheric Science, University of Leeds, Leeds, UK.
[3]UK Met Office, Exeter, UK.
[4]Office National de Météorologie, Algiers, Algeria.
[5]Climate Research Lab, Oxford University Centre for the Environment, Oxford, UK.

Corresponding author: L. Garcia-Carreras, School of Earth and Environment, University of Leeds, Leeds, LS31DL, UK. (eelgc@leeds.ac.uk)

0094-8276/13/10.1002/grl.50239

[3] Numerical models play a significant role in intraseasonal forecasting for West Africa and are therefore a vital tool for the area. Despite the climatic importance of the SHL, there are no routine observations made over large areas of the Sahara desert, with most stations and field campaigns having focused on its margins [*Marsham et al.*, 2013a, black crosses in Figures 1a–1d]. As a result, model errors are not constrained, forecast models exhibit significant biases [*Agusti-Panareda et al.*, 2010], and there are large disagreements between analyses [*Marsham et al.*, 2011]. Various studies have demonstrated model errors in the surface energy balance in the Sahara due to the representation of dust [*Tompkins et al.*, 2005; *Haywood et al.*, 2005] and clouds [*Stein et al.*, 2011; *Marsham et al.*, 2013a]. Models must furthermore capture the vertical mixing of heat, water, dust, and momentum through the complex layerings over the Sahara [*Cuesta et al.*, 2009] and the ventilation of the SHL by cooler air from its margins [*Peyrillé and Lafore*, 2007]. This ventilation can take the form of synoptic scale or mesoscale flows [*Grams et al.*, 2010]. Cold pool outflows from moist convection also appear to ventilate the SHL, especially those emerging from mesoscale convective systems (MCSs) in the Sahel to the south [*Flamant et al.*, 2009; *Bou Karam et al.*, 2008; *Marsham et al.*, 2008; 2013a], but also from the Atlas to the northwest [*Knippertz et al.*, 2009].

[4] Although parameterizations of convection generate cold air at low levels, the parameterized up- and downdrafts are assumed to occur within a model column, and MCSs and their associated cold pools, which in the Sahel can frequently cover many columns in a global forecast model, are poorly represented (see *Moncrieff* [2010], for a review of the issues with the representation of MCSs in global models). Cold pool winds are essentially missing, leading to large errors in dust in global models, but also perhaps contributing to biases in modeled ventilation of the SHL region [*Marsham et al.*, 2011]. In the central Sahara, the stable nocturnal boundary layer masks much of the temperature deficit of many cold pools in surface measurements, e.g., *Hobby et al.* [2012] shows this resulting in a cold pool generating a surface warming. Despite this, near-surface observations from Bordj Badji Mokhtar, Algeria, showed that cold pools produced changes in surface properties of up to 5 K and 4 g kg^{-1} during June 2011 [*Marsham et al.*, 2013a]. One of the two Fennec supersites was located in Bordj Badji Mokhtar, Algeria (BBM) [*Marsham et al.*, 2013a, Figures 1a–1d, black star]. BBM is within the climatological location of the SHL and the maximum mean aerosol optical depth in summer [*Prospero et al.*, 2002]. During the Fennec intensive observation period (IOP), the station was frequently affected by cold

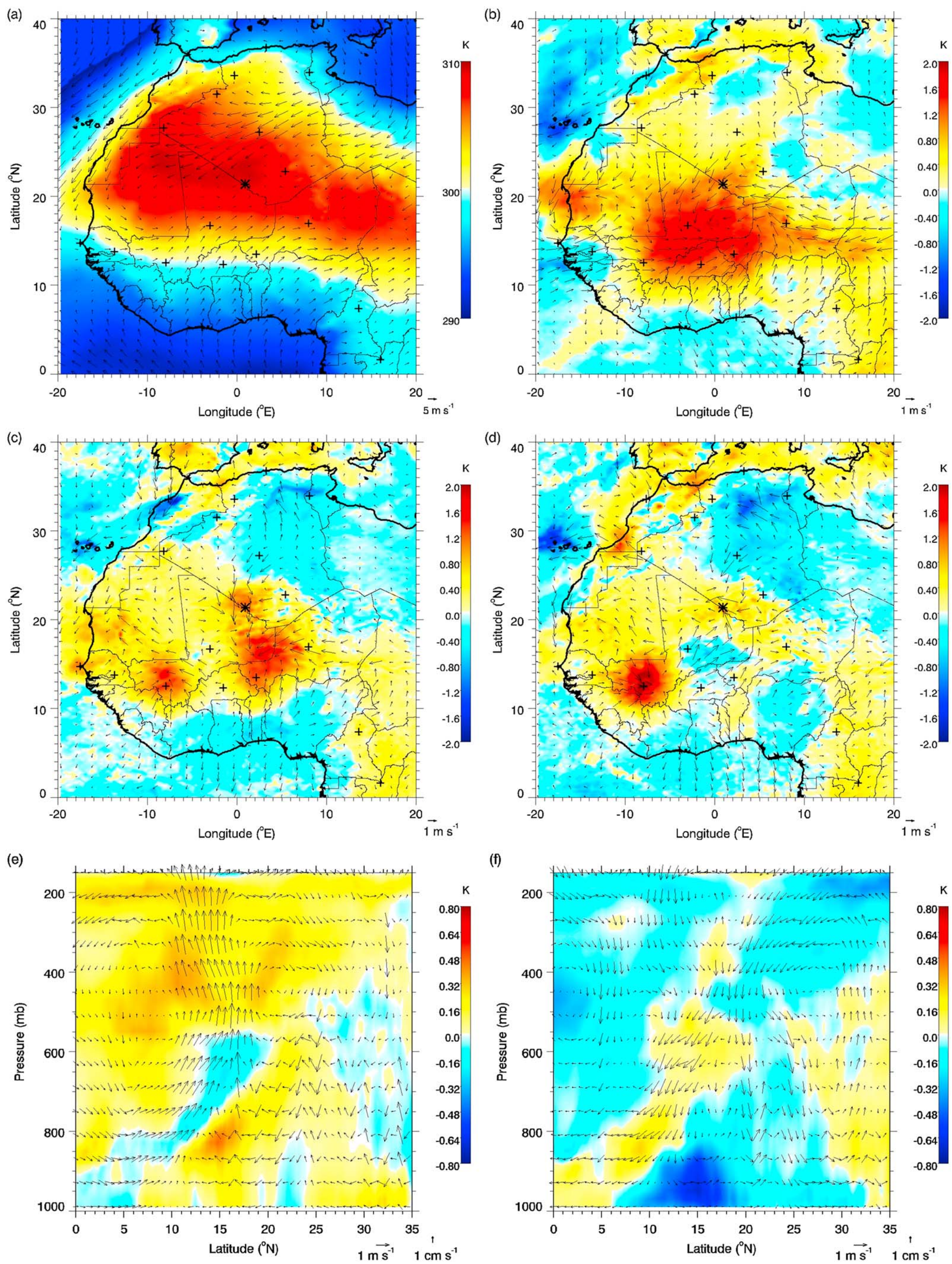

Figure 1. Global UM data averaged between 8 and 30 June 2011. 925-hPa temperature (a) analysis, (b) day + 2 forecast-analysis. Midnight (T + 12) forecast-analysis for (c) days with cold pools (9 days) and (d) days without cold pools (7 days). Potential temperature (colors) and winds (north-south and vertical) forecast-analysis averaged between 10°W and 5°E at (e) 1800 UTC and (f) 0600 UTC. In Figures 1e and 1f forecast data were averaged between day + 1 and day + 3, with biases detrended to remove the lead-time bias and leave the diurnal bias. The star in Figures 1a–1d shows the location of BBM and the crosses show all other African radiosonde stations that were operational during the study period.

pool outflows, largely from moist convection farther south [*Marsham et al.*, 2013a]. Here we use **data** from BBM to confront for the first time model behavior in the remote Sahara with regular in situ profile observations, evaluate the impact of data assimilation on model analyses, and in particular evaluate how cold pool outflows contribute to model biases.

2. Model and Synoptic Conditions

[5] Analysis and forecast data from the operational version of the global Met Office Unified Model (UM, GA3.0, version UM8.0) are compared with BBM IOP Fennec data. The UM, with ~30 km horizontal grid spacing and 70 vertical levels with the lowest level at 20 m, is used

for both weather and climate prediction. Moist convection is parameterized [*Walters et al.*, 2011]. Model data are available at 00, 06, 12, and 18 UTC. All forecasts here are initialized at 12 UTC.

[6] During the main Fennec IOP in June 2011 radiosondes were launched every 3–6 h from BBM (21.4°N, 0.9°E, 420 m above mean sea level, solar noon at 11:57 UTC) and transmitted via the Global Telecommunication System for assimilation by operational centers. For each radiosonde, the UM model "first guess" (a short term forecast before observations are assimilated) and the analysis were stored. Cold pools at BBM were identified subjectively using in situ and satellite data as in *Marsham et al*. [2013a].

[7] June 2011 at BBM was characterized by two distinct periods; a dry period before 13 June with dry Harmattan winds and no cold pools, followed by a period with repeated monsoon surges and cold pools [*Marsham et al*., 2013a]. Due to the lack of cold pools before 13 June, only data for 13–30 June are used in this study unless otherwise stated.

3. Results

3.1. Biases in the UM NWP

[8] During the study period, the monsoon system is well established, with the SHL centered close to 24°N and the monsoon flow reaching all the way to the Sahel (Figure 1a). There is a northward incursion of the monsoon flow just south of BBM (up to ~20°N) leading to the large number of cold pool outflows that are observed at BBM (black star). The 2-day forecast is too warm throughout most of the West African region (Figure 1b). In the center of the SHL, the bias is of 0.5 K, despite the lack of observations. This error is increased to 1 K around BBM, as well as close to other observational stations in the margins of the desert (e.g., Nouakchott, 18.1°N, 16.0°W). The largest biases are observed south of BBM, and results in this paper suggest that these are related to an underestimation of large, organized MCSs in the model, a common issue with convective parameterizations [e.g. *Pearson et al*., 2010]. The SHL is also too dry and deep (0.4 g kg^{-1} and 1 hPa at BBM in the day + 2 forecast, not shown). These biases affect the regional-scale WAM circulation, strengthening the north-south pressure gradient and therefore the monsoon flow (Figure 1b). This in turn affects clouds, precipitation, and the continental water cycle. The biases appear within the first 6 h of the forecast (not shown), suggesting that rapid processes are at least partially responsible for the errors. Similar biases have also been observed in a number of weather and climate models in the past [*Thorncroft et al*., 2003; *Agusti-Panareda et al*., 2010]

[9] When cold pools occur, the midnight warm bias around BBM is greatly enhanced compared to days without cold pools (Figures 1c–1d). The size of the anomaly over BBM (~5°) is indicative of the spatial extent of the impact of assimilating radiosondes in a data sparse region. Similar increases in error around radiosonde stations can be observed at Bamako (12.5°N, 8.0°W), Niamey (13.5°N, 2.2°W), and to a lesser extent Dakar (14.7°N, 17.5°W). The presence of a large positive bias south of BBM only on cold pool days is further evidence that these errors are associated with convection to the south of BBM.

[10] The diurnal cycle of the bias is also consistent with the misrepresentation of convective processes in the model. There is a marked diurnal cycle in cold pools, as these are generated by evaporation of precipitation, which peaks in the evening. Cold pools are also more robust at night, as they are not eroded by dry convection [*Ross et al*., 2004]. At 18 UTC, there is a peak in the warm bias centered at 400 hPa south of 23°N, consistent with too much convection near midday in the forecast (Figure 2e). The low-level warm bias at 15°N, on the other hand, is consistent with the lack of cold pools in the model. At 06 UTC, these two errors are reversed (Figure 2f). In reality, convection peaks late in the evening and can persist throughout the night, while the minimum in the parameterized model convection is at night [*Stratton and Stirling*, 2012], producing an upper level cold bias. The increased strength of the nighttime monsoon flow in the forecast (Figure 1b) then leads to a low-level cold bias at 06 UTC.

[11] In summary, the UM has a warm, dry bias in the SHL that starts to develop within the first 6 h of the simulation. This bias in turn produces too strong a regional scale monsoon circulation. Although the cause and effect cannot be determined from the model output alone, the low-level model biases near BBM are larger on days with cold pools and are consistent with known errors in the diurnal cycle of parameterized convection.

3.2. Impacts of Assimilation

[12] In order to evaluate the contribution of cold pools to model biases in Figure 1, the errors in the model first guess (solid lines) and the analysis (dashed lines) compared to the assimilated radiosonde observations are shown in Figure 2. These are computed for all radiosondes (black, 99 sondes) and only for radiosondes that were (blue, 19 sondes) and were not (red, 80 sondes) affected by cold pools. A simple linear regression of model error against a factor (cold pool) is used to quantify the contribution of cold pools to the mean error. Although this assumes that all cold pools are the same, while their properties are observed to vary, it provides a useful quantification of the mean contribution of cold pools to the model errors shown in Figure 2. Table 1 shows observations (O) in cold pools (cp) and not in cold pools (ncp), the errors in the model first guess (FG-O) and the analysis (A-O) at 925 hPa when there are no cold pools (ncp), and the *additional* error when cold pools are present (acp). Errors are shown for all times, as well as using only data between 18 to 00 UTC (contributing to the midnight analysis, columns marked 00 UTC). Errors that are not significant to the 5% level are recorded as zero.

[13] The total errors in the model first guess (Figure 2, black solid line) are consistent with the biases shown in Figure 1, with the model boundary layer being on average 0.6 K too warm and 2% too dry (10% of total) in relative humidity (Figures 2a–2b). Although cold pools affected only 20% of all radiosonde observations, the temperature and humidity errors are increased by factors of 4.5 and 2.5, respectively, within cold pools compared to non cold-pool events, thus contributing to the majority of the mean error. The meridional humidity flux bias shows the impact of temperature (and thus wind) and humidity errors on the regional scale water budget and circulation. Cold pools increase the meridional humidity flux by a factor of 3 compared to when cold pools are not present (Table 1, observations) and are responsible for 29% of the total

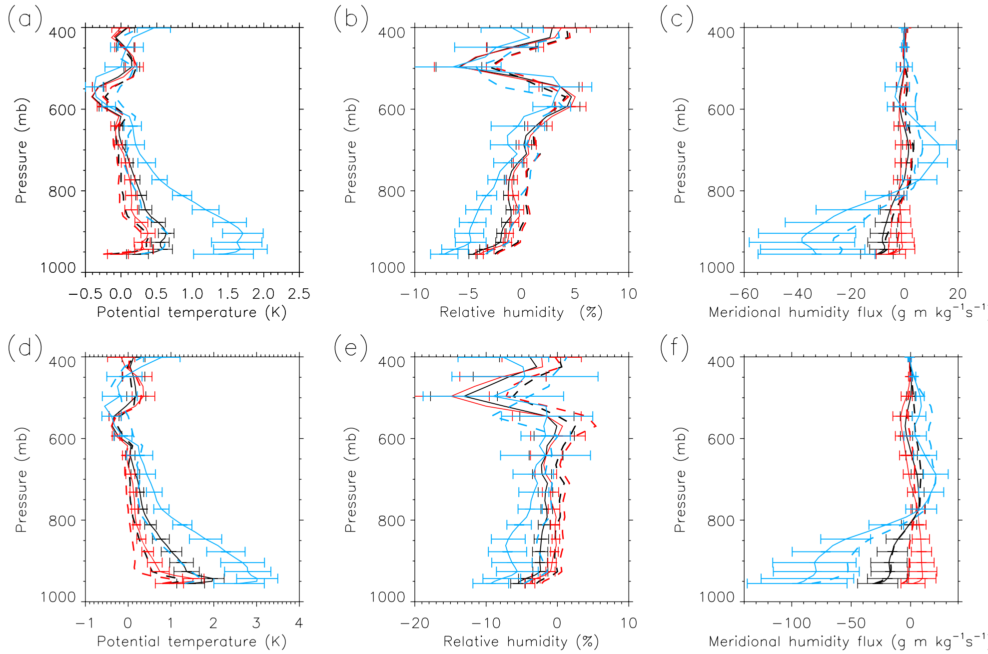

Figure 2. Data assimilation statistics from the BBM radiosonde station between 8 and 30 June 2011. Profiles of models (solid line) first guess–observations and (dashed line) analysis-observations averaged for all data points (black, 99 sondes) and days when cold pools were (blue, 19 sondes) and were not (red, 80 sondes) observed of (a) potential temperature, (b) relative humidity, and (c) meridional humidity flux. (d–f) Same as Figures 2a–2c, but only using radiosondes launched between 18 and 00 UTC. Error bars show the standard error and are only included for the model first guess for clarity.

observed flux. As this contribution is missing in the model, the mean bias is similarly of 28%.

[14] The vertical structure of the errors is consistent with the structure of cold pools. Observations show squall lines can generate cold, moist air below ~4 km [*Bryan and Parker*, 2010], consistent with the cold pool temperature error up to 600 hPa. Rear to front flow is seen in the lower portion of this cold air in *Bryan and Parker* [2010], with system-relative front to rear flow above, consistent with the negative flux error below 700 hPa and the positive error between 700 and 600 hPa.

[15] The analyses (Figure 2, dashed lines), as would be expected, are closer to the observations than the model first guess in all cases. Although analysis errors remain larger in the presence of cold pools, the differences are not statistically significant for temperature and humidity. The meridional humidity flux on the other hand is 18% too low in the analysis solely due to errors during cold pool events. It is also worth noting that the BBM radiosonde station was only operational during the Fennec IOP, so the model first guess is likely to be a better estimate of the errors usually present in the operational version of the UM.

[16] Due to the observed diurnal cycle in cold pools, their absence affects the diurnal cycle in the model, as well as the mean biases. This is particularly important in the WAM region, which is also characterized by a strong diurnal cycle in heating and circulation: during the day, convection suppresses the large-scale flow, while at night and early hours of the morning, the monsoon flow can accelerate, transporting moisture inland [*Parker et al.*, 2005]. Figures 2d–2f show errors for radiosondes launched between 18 and 00 UTC. Cold pools again contribute to the majority of the total errors observed, but magnitudes are substantially increased. For temperature, the error increases both in cold pool and non cold-pool events, but errors within cold pools are nearly 3 times larger. There is a peak in temperature error immediately above the surface, particularly when cold pools were not present. This is likely

Table 1. Mean Model Errors With and Without Cold Pools[a]

		Temperature (K)		Relative Humidity (%)		Meridional Humidity Flux (g m kg^{-1} s^{-1})	
		All	00 UTC	All	00 UTC	All	00 UTC
O	ncp	308 ± 0.2	309.4 ± 0.4	14.9 ± 0.7	12 ± 1	19 ± 9	0
	cp	307.3 ± 0.6	307.0 ± 0.8	18.2 ± 2.0	19 ± 3	57 ± 24	120 ± 40
FG-O	ncp	0.29 ± 0.12	0.72 ± 0.26	−1.35 ± 0.46	0	0	0
	acp	1.30 ± 0.28	2.01 ± 0.47	−3.4 ± 1.1	−4.6 ± 2.1	–37 ± 14	−89 ± 30
A-O	ncp	0.29 ± 0.02	0	0	0	0	0
	acp	0	1.28 ± 0.40	0	0	−24 ± 9	−52 ± 14

[a]Mean 925 hPa observations (O), model first guess–observation (FG-O), and analysis-observation (A-O) averaged for all times and only for sondes that went into the midnight analysis (00 UTC), split between non cold-pool (ncp) and cold pool (cp/acp) events. The cold pool errors are the additional error caused by the presence of cold pools. Errors that are not significant to the 5% level are recorded as zero.

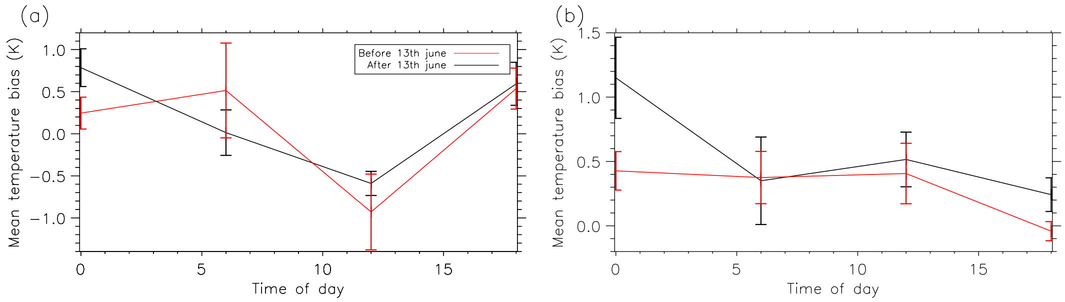

Figure 3. Diurnal cycle of 925 hPa temperature in (a) model first guess–observations and (b) day + 1 forecast–analysis averaged for (red) the period 1–12 June 2011 and (black) the period 13–30 June. The radiosonde data only begins on 8 June.

due to issues with the representation of the nocturnal boundary layer, which is sensitive to the surface state and so difficult to accurately reproduce in models. This peak is less obvious within cold pools where surface air is mixed vertically. Relative humidity and meridional humidity flux errors average to zero without cold pools but have errors of 24% and 74% of the total respectively in the presence of cold pools. Due to the larger magnitudes in the errors at night, the analysis also significantly deviates from observations during cold pool events. These errors are comparable to those shown in Figure 1, implying that nighttime forecast biases are underestimated due to biases present in the analysis.

[17] To further understand the driving mechanism of the errors in Figure 2, the diurnal cycle in the model first guess error for the periods before and after 13 June (without and with cold pools, respectively) can be compared. The errors are not statistically different between the two time periods except at midnight, where the error is maximised after 13 June, consistent with model biases caused by cold pools (Figure 3a). A similar picture emerges from the day + 1 forecast biases. Although there is a warm bias throughout the month at all times, there is a pronounced peak in the error at midnight only after 13 June (Figure 3b).

[18] The absence of propagating cold pools represents only one issue with parameterized convection, which also produces biases in the timing and distribution of convection, thus affecting the diurnal cycle of radiation, surface fluxes, and in turn the regional scale circulation [*Marsham et al.*, 2013b; *Moncrieff*, 2010; *Stratton and Stirling*, 2012]. Furthermore, cold pools are associated with dust uplift [*Marsham et al.*, 2011] and subsequent initiation of clouds, all of which will also contribute to model biases. The results shown in Figure 2, however, are all mutually consistent with missing advective cooling in terms of the signs of the errors (too warm and dry with too little advection from the south), their magnitude (e.g., *Marsham et al.*, 2013a), vertical structure and diurnal cycle. It would be difficult to reconcile all these features invoking other processes as primary mechanisms. For example, radiative impacts due to missing dust or cloud associated with cold pools would be expected to lead to low-level warming at night, not cooling as is observed. Errors in the large-scale circulation, on the other hand, would be unlikely to correlate with cold pool events at one single station, as these would be dependent on the representation of convection throughout the whole region. Figure S1 shows the model and observed profiles before and after the passage of a cold pool, as identified by satellite imagery. These show that, for a specific, identifiable, cold pool event, the model errors are very similar to the mean profiles shown in Figure 2, providing further evidence that the driving mechanism of the error is the missing advective cooling and moistening from propagating cold pools (see section S1 for further details).

4. Discussion and Conclusions

[19] Radiosonde data and data assimilation statistics from Fennec supersite 1 at Bordj Badji Mokhtar (Algeria) in the remote Sahara have been used to evaluate the impact of convectively-generated cold pools on model errors in the SHL region. The model first guess, which represents a short-term forecast, is too warm and dry in all cases, but the errors are larger by a factor of 3–5 when cold pools occur. These errors are significantly larger at midnight, when cold pools are most intense, producing a diurnal cycle in the bias which in turn affects the diurnal cycle in the model.

[20] The observations show that cold pools generate 29% of the observed meridional humidity flux, but this contribution is completely absent in the model, thus affecting the large-scale water cycle of the WAM/SHL system.

[21] Assimilating the radiosonde data substantially reduces the errors in the analysis, but cold pools still cause significant biases of 1.3 K in temperature and $-50\,\mathrm{g\,m\,kg^{-1}\,s^{-1}}$ (42% of the total) in the meridional humidity flux at night. Furthermore, the BBM radiosonde station was only operational for the duration of the Fennec IOP, and very few operational stations exist close to the SHL, meaning that the first-guess errors are likely to be more typical for operational UM runs.

[22] This study provides a case for more routine observations in and around the Sahara in order to better constrain analyses, which exhibit large differences between models [*Marsham et al.*, 2011]. Figures 1c–1d also highlight another issue that arises from the scarcity of radiosonde stations in the region: data assimilation systems work best with dense observational networks and the influence of BBM data extends approximately 5° with no clear influence of any sonde data beyond this, until the next sounding location is reached. This is not representative of the real impact of cold pools, which can spread over much larger areas and generally move northward (as the convection lies farther south). Considered another way, a single point measurement is unlikely to be representative for such a large area, so isolated stations may have an excessive impact on the analysis. Spurious temperature gradients are also created around radiosonde stations in the model, affecting winds and cloud cover locally [*Agusti-Panareda et al.*, 2010].

Due to the large errors observed during cold pool events, this issue is particularly problematic in the Sahara and may be sensitive to the data assimilation technique used.

[23] Errors from cold pools are caused by systematic errors in both the modeled moist convection and the associated cold pools in global models. Convective parameterizations consider each model column independently, so cold pools are a particular challenge as they span multiple grid boxes. The errors quantified here are consistent with model biases found in the global UM operational forecast model over the central Sahara, suggesting that cold pools are, at the very least, one contributing factor to large-scale biases in the region. Quantifying the extent of this contribution, relative to errors arising from other deficiencies of parameterizations of convection, should be a priority for future research. These errors are likely to be important for the vast majority of operational global models, since these all use parameterized convection. Explicit convection in global models will not be feasible in the foreseeable future. This study highlights the need to implement a cold pool parameterization, such as the one described by [*Grandpeix and Lafore*, 2010], in weather and climate models, which depend on parameterized convection.

[24] The mountains to the north-east and south-east of BBM mean that it is probably unusually influenced by cold pools, but cold pools are observed to ventilate the Sahara all along its northern and southern boundaries. The results provide observational evidence that the misrepresentation of the upscale impacts of moist convection in the model are a significant factor contributing to continental scale biases, affecting the West African monsoon circulation, as also shown in *Marsham et al.* [2013b].

[25] **Acknowledgments**. Fennec was funded by a NERC consortium grant (NE/G017166/1). We would like to thank Benyakoub Abderrahmane, Mohammed Limam, and Diali Sidali (ONM) for assisting with the Fennec supersite and indeed all at ONM. We would also like to thank Colin Parrett for providing the data assimilation statistics and Lawrence Jackson for help with the statistical analysis.

References

Agusti-Panareda, A., et al. (2010), Impacts of assimilating AMMA soundings on ECMWF analyses and forecasts, *Weather Forecast*, *25*(4), 1142–1160.

Bou Karam, D., et al. (2008), Dust emissions over the Sahel associated with the West African monsoon intertropical discontinuity region: A representative case-study, *Q. J. R. Meteorol. Soc.*, *134*(632), 621–634.

Bryan, G., and M. Parker (2010), Observations of a squall line and its near environment using high-frequency rawinsonde launches during VORTEX2, *Mon. Wea. Rev.*, *138*, 4076–4097.

Cuesta, J., et al. (2009), Dynamical mechanisms controlling the vertical redistribution of dust and the thermodynamic structure of the west Saharan atmospheric boundary layer during summer, *Atmos. Sci. Lett.*, *10*(1), 34–42.

Flamant, C., et al. (2009), The impact of a mesoscale convective system cold pool on the northward propagation of the intertropical discontinuity over West Africa, *Q. J. R. Meteorol. Soc.*, *135*(638), 139–159.

Grams, C., et al. (2010), The Atlantic inflow to the Saharan heat low: Observations and modelling, *Q. J. R. Meteorol. Soc.*, *136*(S1), 125–140.

Grandpeix, J., and J. Lafore (2010), A density current parameterization coupled with Emanuel's convection scheme. Part I: The models, *J. Atmos. Sci.*, *67*(4), 881–897.

Haywood, J., et al. (2005), Can desert dust explain the outgoing longwave radiation anomaly over the Sahara during July 2003?, *J. Geophys. Res.*, *110*(D5), D05,105.

Hobby, M., et al. (2012), The Fennec Automatic Weather Station (AWS) Network: Monitoring the Saharan Climate System, *J. Atmos. Ocean. Technol.*, doi:10.1175/JTECH-D-12-00037.1.

Knippertz, P., et al. (2009), High-resolution simulations of convective cold pools over the northwestern Sahara, *J. Geophys. Res.*, *114*(D8), D08,110.

Marsham, J., et al. (2008), Uplift of Saharan dust south of the intertropical discontinuity, *J. Geophys. Res.*, *113*(D21), D21,102.

Marsham, J., et al. (2011), The importance of the representation of deep convection for modeled dust-generating winds over West Africa during summer, *Geophys. Res. Lett.*, *38*(16), L16,803.

Marsham, J. H., et al. (2013a), Meteorology and dust in the central sahara: Observations from fennec supersite-1 during the June 2011 intensive observation period, *J. Geophys. Res. Atmos.*, doi:10.1002/jgrd.50211.

Marsham, J. H., et al. (2013b), The role of moist convection in the West African monsoon system - insights from continental-scale convection-permitting simulations, *Geophys. Res. Lett.*, doi:10.1002/grl.50347.

Moncrieff, M. W. (2010), The multiscale organization of moist convection and the intersection of weather and climate, in Climate Dynamics: Why Does Climate Vary? Geophys. Monogr. Ser., vol. *189*, edited by D.-Z. Sun, and F. Bryan, pp. 3–26, AGU, Washington, D.C., , doi:10.1029/GM189.

Parker, D. J., et al. (2005), The diurnal cycle of the West African monsoon circulation, *Q. J. R. Meteorol. Soc.*, *131*(611), 2839–2860.

Pearson, K., et al. (2010), Evaluation of the model representation of the evolution of convective systems using satellite observations of outgoing longwave radiation, *J. Geophys. Res. Atmos.*, *115*(D20), D20,206.

Peyrillé, P., and J. Lafore (2007), An idealized two-dimensional framework to study the West African monsoon. Part II: Large-scale advection and the diurnal cycle, *J. Atmos. Sci.*, *64*(8), 2783–2803.

Prospero, J., et al. (2002), Environmental characterization of global sources of atmospheric soil dust identified with the Nimbus 7 Total Ozone Mapping Spectrometer (TOMS) absorbing aerosol product, *Rev. Geophys*, *40*(1), 1002.

Ramel, R., H. Gallee, and C. Messager (2006), On the northward shift of the West African monsoon, *Clim. Dynam.*, *26*(4), 429–440.

Ross, A., et al. (2004), Simple models of the role of surface fluxes in convective cold pool evolution, *J. Atmos. Sci.*, *61*(13), 1582–1595.

Stein, T., et al. (2011), The vertical cloud structure of the West African monsoon: A four-year climatology using Cloudsat and Calipso, *J. Geophys. Res. Atmos.*, *116*, D22,205

Stratton, R., and A. Stirling (2012), Improving the diurnal cycle of convection in GCMs, *Q. J. R. Meteorol. Soc.*, *138*, 1121–1134, doi: 10.1002/qj.991.

Thorncroft, C. D., et al. (2003), The JET2000 project – Aircraft observations of the African easterly jet and African easterly waves, *Bull. Amer. Metetorol.*, *84*, 337–351.

Tompkins, A., et al. (2005), Influence of aerosol climatology on forecasts of the African Easterly Jet, *Geophys. Res. Lett.*, *32* (10), L10,801.

Walters, D., et al. (2011), The Met Office Unified Model global atmosphere 3.0/3.1 and JULES global land 3.0/3.1 configurations, *Geosci. Model Dev.*, *4*, 919–941.